In vivo ratiometric Zn2+ imaging in zebrafish larvae using a new visible light excitable fluorescent sensor

ARTICLE *in* CHEMICAL COMMUNICATIONS · DECEMBER 2013

Impact Factor: 6.83 · DOI: 10.1039/c3cc46262e · Source: PubMed

7 AUTHORS, INCLUDING:

Zhipeng Liu
Nanjing Tech Universtiy
27 PUBLICATIONS **678** CITATIONS
SEE PROFILE

Changli Zhang
Nanjing Xiaozhuang University
22 PUBLICATIONS **862** CITATIONS
SEE PROFILE

Yuncong Chen
The Hong Kong University of Science and T…
17 PUBLICATIONS **287** CITATIONS
SEE PROFILE

Weijiang He
Nanjing University
66 PUBLICATIONS **1,507** CITATIONS
SEE PROFILE

ChemComm

COMMUNICATION

View Article Online
View Journal | View Issue

Cite this: *Chem. Commun.*, 2014, **50**, 1253

Received 15th August 2013,
Accepted 25th November 2013

DOI: 10.1039/c3cc46262e

www.rsc.org/chemcomm

In vivo ratiometric Zn^{2+} imaging in zebrafish larvae using a new visible light excitable fluorescent sensor†

Zhipeng Liu,‡[ab] Changli Zhang,‡[ac] Yuncong Chen,[a] Fang Qian,[a] Yang Bai,[a] Weijiang He*[a] and Zijian Guo*[a]

A visible light excitable ratiometric Zn^{2+} sensor was developed by integrating a Zn^{2+} chelator as the ICT donor of the fluorophore sulfamoylbenzoxadiazole, which displays the Zn^{2+}-induced hypsochromic emission shift (40 nm) and favors the *in vivo* ratiometric Zn^{2+} imaging in zebrafish larvae.

Labile Zn^{2+} is attracting growing interest since it is associated with both physiological processes such as neurotransmission and gene transcription,[1] and the pathophysiology of certain diseases.[2] Fluorescent Zn^{2+} imaging with Zn^{2+} sensors has demonstrated great success in providing temporal–spatial information regarding the Zn^{2+} homeostasis in live cells.[3] Since cellular Zn^{2+} biology is far from the complicated Zn^{2+} physiology in advanced organisms, the *in vivo* Zn^{2+} imaging in living animal models is especially demanded. As a valuable vertebrate model of high homology with mammals, the zebrafish embryo or larva benefits the studies of developmental biology, molecular genetics, neuroscience, signal transduction, and pathology due to its small size and optical transparency for *in vivo* imaging.[4] Moreover, the controlled external fertilization enables the *in vivo* imaging during all stages of embryonic development. Therefore, development of Zn^{2+} sensors especially those having long excitation wavelengths to promote *in vivo* Zn^{2+} imaging in zebrafish larvae is one of the most interesting areas in this field, and several turn-on sensors have been applied for Zn^{2+} imaging in live zebrafish larvae after our first report.[5] However, this turn-on *in vivo* Zn^{2+} imaging still suffers from the interference induced by altered sensor concentration, autofluorescence, bleaching, *etc.* A more accurate Zn^{2+} imaging method for zebrafish larvae is ratiometric Zn^{2+} imaging demanding the ratiometric Zn^{2+} sensors of visible light/NIR excitability.

In this communication, we report a visible light excitable ratiometric Zn^{2+} sensor **SBD-TPEA**, which has been utilized for the first *in vivo* ratiometric Zn^{2+} imaging in zebrafish larvae. This sensor was constructed using a mechanism of metal coordination altering the ICT (intramolecular charge transfer) effect in fluorophores, which is an effective design rationale for ratiometric metal ion sensors.[6] In this sensor, the Zn^{2+} chelator, **TPEA** (*N,N,N′*-tri(pyridin-2-ylmethyl)-ethane-1,2-diamine), was incorporated into an ICT fluorophore **ASBD** (4-amine-7-sulfamoylbenzo[*c*][1,2,5]oxadiazole) acting as both the ICT donor group and Zn^{2+} ionophore. This sensor was prepared in a moderate yield by reacting **SBD-Cl** with **TPEA** *via* a SN_{Ar} substitution (Scheme 1, please see also ESI†).

The sensor can be dissolved in water with a concentration of up to ~3.0 μM according to a reported determination procedure (Fig. S7, ESI†).[7] The spectroscopic determination of **SBD-TPEA** was carried out in HEPES buffer (50 mM HEPES, 100 mM KNO_3, pH 7.2) containing 0.15% DMSO. **SBD-TPEA** exhibits an emission band centered at 585 nm, with an excitation maximum at 466 nm. The large Stokes shift (119 nm) is helpful in reducing the excitation interference in imaging. Fluorescence Zn^{2+} titration of **SBD-TPEA** displayed a distinct hypsochromic emission shift from 585 to 545 nm with an isoemission point at 585 nm (Fig. 1a). The ratio of emission at 545 nm to that at 585 nm (F_{545}/F_{585}) increases linearly from 0.85 to 1.42 with $[Zn^{2+}]_{total}$ until the $[Zn^{2+}]_{total}$/[**SBD-TPEA**] ratio attains the value 1 : 1 (Fig. 1b). A higher $[Zn^{2+}]_{total}$ does not lead to

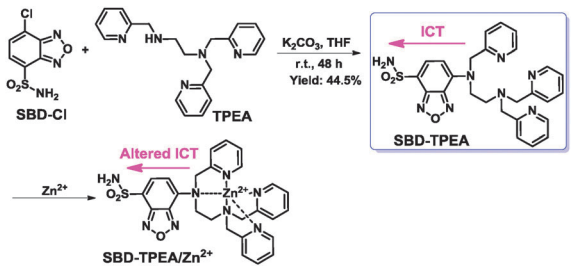

Scheme 1 Synthesis of **SBD-TPEA** and its Zn^{2+} complexation.

[a] *State Key Laboratory of Coordination Chemistry, Coordination Chemistry Institute, School of Chemistry and Chemical Engineering, Nanjing University, Nanjing 210093, P. R. China. E-mail: heweij69@nju.edu.cn, zguo@nju.edu.cn; Fax: +86 25 83314502; Tel: +86 25 83597066*

[b] *Department of chemistry, Liaocheng Unviersity, Liaocheng, 252059, P. R. China*

[c] *Department of chemistry, Nanjing Xiaozhuang College, Nanjing, 210017, P. R. China*

† Electronic supplementary information (ESI) available: Synthesis of **SBD-TPEA**, spectroscopic studies and experimental details. See DOI: 10.1039/c3cc46262e

‡ Both authors contributed equally to this manuscript.

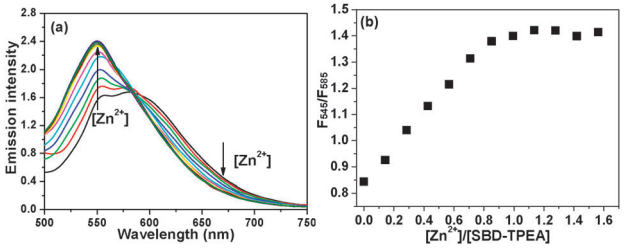

Fig. 1 (a) Emission spectra of 3 μM **SBD-TPEA** (λ_{ex}, 460 nm) in HEPES buffer (50 mM, 0.1 M KNO_3, pH 7.2, containing 0.15% DMSO) obtained by adding aliquots of Zn^{2+} solution (1.2 mM, 1.1 μL); (b) the titration profile according to the ratio of emission at 545 nm to that at 585 nm, F_{545}/F_{585}.

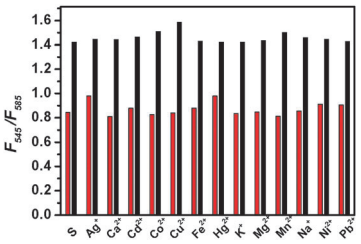

Fig. 2 Ratio of emission at 545 to that at 585 nm, F_{545}/F_{585}, of **SBD-TPEA** (3 μM) in HEPES buffer (0.15% DMSO, 50 mM HEPES, 100 mM KNO_3; pH 7.20) induced by different metal cations. Red bars, ratio for free sensor (S) or in the presence of 1 equiv. Ag^+, Cd^{2+}, Co^{2+}, Cu^{2+}, Fe^{2+}, Hg^{2+}, Mn^{2+}, Ni^{2+}, Pb^{2+} or 1000 equiv. Na^+, K^+, Ca^{2+}, Mg^{2+}. Black bars, ratio in the presence of Zn^{2+} (1 equiv.), or the indicated metal ions (1 equiv.) followed by adding 1 equiv. Zn^{2+}. λ_{ex}, 460 nm.

any evident change in emission. The excitation and emission maxima for both apo- and Zn^{2+}-bound sensors are located in the range of visible light, favouring *in vivo* imaging in zebrafish larvae. Fluorescence pH titration demonstrated that F_{454}/F_{585} of **SBD-TPEA** has no pH-dependence in the pH range from 6.5 to 9.0, favoring its ratiometric imaging application in physiological microenvironments (Fig. S8, ESI†). In addition, the Zn^{2+}-induced emission enhancement for **SBD-TPEA** is limited, suggesting that there is no distinct PET (photo-induced electron transfer) effect from Zn^{2+} ionophores to the parent fluorophore, **ASBD**.[6a]

The UV-vis Zn^{2+} titration of **SBD-TPEA** demonstrated an absorption shift from 456 (band A, ε, 4.46×10^3 M^{-1} cm^{-1}) to 386 nm (band B, ε, 3.29×10^3 M^{-1} cm^{-1}, Fig. S9, ESI†). The linear decrease of band A and increase of band B with $[Zn^{2+}]_{total}$ can be observed simultaneously till the $[Zn^{2+}]_{total}$/[**SBD-TPEA**] ratio attains the value 1 : 1. A higher zinc concentration does not lead to any further change. The UV-vis titration profiles according to the absorbance of the two bands and the clear isosbestic point at 416 nm suggest that Zn^{2+} addition led to only one reaction to form the sole Zn^{2+} complex of 1 : 1 stoichiometry. ^1H NMR titration by Zn^{2+} also confirmed the 1 : 1 Zn^{2+} binding stoichiometry of **SBD-TPEA** (Fig. S10, ESI†), and all N atoms in **TPEA** are involved in Zn^{2+} coordination directly (Fig. S10–S12, Table S1 and Chart S1, ESI†). MS determination of the **SBD-TPEA**–Zn^{2+} complex again confirmed the 1 : 1 Zn^{2+} binding stoichiometry (Fig. S6, ESI†). The data obtained from the two Zn^{2+} titrations implied that Zn^{2+} coordination to **TPEA** amine N attached to benzoxadiazole decreases the ICT effect of **ASBD** fluorophore and induces the hypsochromic shift of absorption and emission.

The Zn^{2+}-specific ratiometric response of **SBD-TPEA** was confirmed further by fluorescence titration with biorelated metal cations of interest. As shown in Fig. 2, the presence of Na^+, K^+, Ca^{2+}, and Mg^{2+}, which are abundant in cells, does not interfere with its ratiometric response to Zn^{2+}, even though their concentration is 1000 times higher than $[Zn^{2+}]_{total}$. In addition, the presence of Ag^+, Fe^{2+}, Hg^{2+}, Ni^{2+}, Mn^{2+} Co^{2+}, Cd^{2+}, Cu^{2+}, and Pb^{2+} (1 equiv.) does not interfere with its ratiometric sensing ability for Zn^{2+}. The K_d value of the Zn^{2+}–**SBD-TPEA** complex was estimated to be ~2.1 nM *via* determination of the Zn^{2+}-induced change of F_{545}/F_{585} ratio in a series of Zn^{2+} buffer solutions (Fig. S13, ESI†).[8] The detection limit (3σ/slope) of this sensor was determined to be 0.5 nM (Fig. S14, ESI†). All these make **SBD-TPEA** a suitable candidate of ratiometric imaging agent for intracellular and *in vivo* Zn^{2+}.

The intracellular Zn^{2+} imaging ability of **SBD-TPEA** was investigated in HepG2 cells using a confocal microscope in a dual emission mode (green channel: 510–560 nm; red channel: 580–630 nm) upon excitation at 488 nm, and the ratiometric images were obtained by mediating the green channel image with the related red channel image (Fig. S15, ESI†). As shown in Fig. 3, the cells stained by **SBD-TPEA** display the faint green/blue (lower ratio) in cytoplasm in the ratiometric image, indicating that the labile Zn^{2+} level in cytoplasm is low. When exogenous Zn^{2+} was introduced *via* incubation the cells with $ZnSO_4$–pyrithione solution (5 μM, 1 : 2), an intense blue color was observed inside the cell, indicating the enhanced intracellular Zn^{2+} level. According the ratio bar, the red/yellow spots close to the nucleus indicate that the Zn^{2+} level in these regions is even higher. The following incubation treatment with the cell membrane permeable Zn^{2+} chelator, *N*,*N*,*N*′,*N*′-tetrakis(2-pyridylmethyl)ethylenediamine (TPEN), displayed a very minor green area inside the cells, implying the distinctly suppressed emission ratio and lower Zn^{2+} level compared to that in the original cells in Fig. 3b. These results also confirmed that the fluorescence ratio enhancement in cells upon $ZnSO_4$–pyrithione incubation was resulted from Zn^{2+} binding of **SBD-TPEA**, and the intracellular Zn^{2+} level can be enhanced effectively *via* Zn^{2+} incubation. Similar results were also obtained in HeLa cells (Fig. S16, ESI†), and the higher Zn^{2+} level was also observed in the regions close to the nucleus when exogenous Zn^{2+} was introduced. Co-localization experiments in HeLa cells (Fig. S17, ESI†) and HepG2 cells *via* co-staining of the cells with **SBD-TPEA** and Golgi marker BODIPY TR ceramide disclosed that the bright spots of

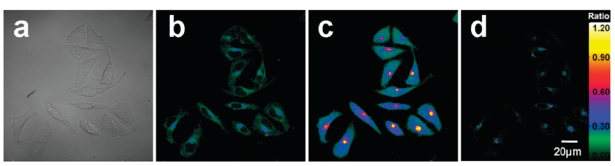

Fig. 3 Confocal fluorescence ratiometric imaging of HepG2 cells stained using **SBD-TPEA** (10 μM, 20 min) at 25 °C. (a) Bright-field transmission image of the stained cells; (b) ratiometric image of cells in (a); (c) ratiometric image of cells in (b) exposed to $ZnSO_4$–pyrithione solution (5 μM, 1 : 2) for 5 min, followed by staining again with **SBD-TPEA** solution; (d) ratiometric image of cells in (c) treated by TPEN solution (25 μM, 10 min). Ratiometric images were obtained *via* mediating of the fluorescence images collected respectively at the green channel (510–560 nm) and the red channel (580–630 nm). λ_{ex}, 488 nm.

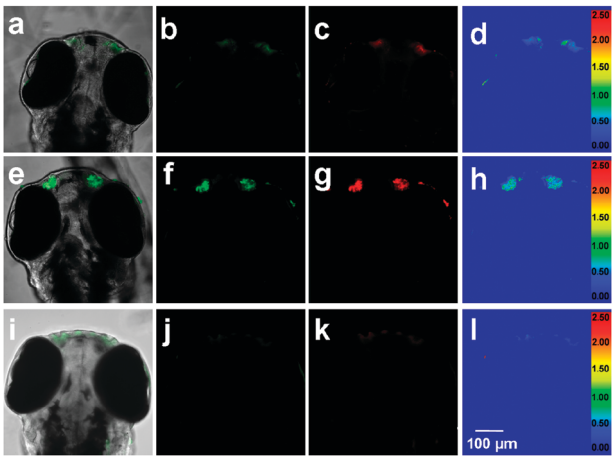

Fig. 4 Confocal fluorescence ratiometric Zn^{2+} imaging in the head of 3-day-old zebrafish larva at 28.5 °C. (a–d) Images of a larva incubated with **SBD-TPEA** (50 μM, 1.5 h); (e–h) images of a larva fed with Zn^{2+} (100 μM, 1 h) solution followed by incubation with **SBD-TPEA** (50 μM, 1.5 h); (i–l) images of a larva incubated with **SBD-TPEA** (50 μM, 1.5 h) followed by 20 min of TPEN incubation (50 μM). (a, e, i) Colocalization of bright-field and fluorescence images for the head (dorsal view); (b, f, j) fluorescence images from the band path 500–560 nm; (c, g, k) fluorescence images from the band path 570–650 nm; (d, h, i) ratiometric images generated from (b, f, j) and (c, g, k). λ_{ex}, 488 nm.

higher Zn^{2+} level are the Golgi apparatus. In addition, the chelatable [Zn^{2+}] in the Golgi of HepG 2 cells was estimated to be around 0.5 nM (Fig. 3 and Fig. S15, ESI†). The ratiometric imaging results also suggest that the average chelatable Zn^{2+} level in HepG2 cells is different from that in HeLa cells. Moreover, the temporal imaging of cells treated by **SBD-TPEA** displayed no change in cell morphology in 4 h, implying the fine biocompatibility of **SBD-TPEA.**

Besides the ratiometric Zn^{2+} imaging ability in living cells of **SBD-TPEA,** the first ratiometric *in vivo* Zn^{2+} imaging in 3-day-old zebrafish larvae was also investigated *via* staining the larvae using **SBD-TPEA** (50 μM, 1.5 h). As shown in Fig. 4a, the confocal fluorescence images of the larva head exhibit mainly two regions of bright fluorescence, and the overlay of fluorescence and bright-field images discloses that two bright regions are symmetrically located between the two eyes, which were proposed to be the neuromasts of the anterior lateral-line system (ALL system) in zebrafish.[9] The ratiometric image obtained *via* mediating fluorescence images obtained respectively from band paths 550–560 and 570–650 nm displays the pale blue regions on the same location, indicating the higher Zn^{2+} level in these two bright spots than that in the rest of the head (Fig. 4a–d). The ratiometric imaging of Zn^{2+}-fed zebrafish larvae (3 day old) has also been carried out by incubating larvae with Zn^{2+} solution for 1 h (100 μM), and the ratiometric image demonstrates two bright cyan spots in the same location (Fig. 4e–h). Moreover, the two cyan regions are larger than the pale blue regions found in the non-Zn^{2+}-fed larvae, and the bright cyan implies that the neuromast Zn^{2+} level in Zn^{2+}-fed larvae is higher than that in non-Zn^{2+}-fed larvae. The **TPEN** (50 μM, 0.3 h) treatment of the **SBD-TPEA** stained 3 day old zebrafish larvae (50 μM, 1.5 h) results in almost dim images and the fluorescence in the neuromast is very low. In addition, only very minor faint pale blue spots can be found in the corresponding areas in the ratiometric image (Fig. 4i–l). A comparison between the ratiometric images of the normal zebrafish larvae and the TPEN treated larvae suggests that the two pale blue regions in the normal zebrafish larvae should be correlated with the presence of higher labile Zn^{2+} levels. All the altered emission ratios displayed as the variable color in the ratiometric image are correlated to the variable chelatable Zn^{2+} levels in live zebrafish larvae. The ratiometric imaging results on 5 zebrafish larvae disclosed that the chelatable [Zn^{2+}] of neuromasts is around 1.3 nM, while the Zn^{2+}-incubation made the [Zn^{2+}] in the corresponding regions increase to 10.9 nM. As for the TPEN treated larvae, the chelatable [Zn^{2+}] in neuromasts can be reduced to 0.1 nM (Fig. S18, ESI†). All the preliminary imaging data indicate that **SBD-TPEA** is an effective Zn^{2+} ratiometric sensor for *in vivo* Zn^{2+} quantitative imaging.

In conclusion, a novel ratiometric Zn^{2+} fluorescent sensor **SBD-TPEA** derived from the ICT fluorophore **ASBD** was developed. This new sensor displays the specific Zn^{2+}-induced emission shift from 585 to 545 nm, which provides the sensor with the ratiometric Zn^{2+} sensing ability. With the pH-independent sensing behavior in the physiological pH range and visible light excitability, **SBD-TPEA** has been utilized to realize the *in vivo* ratiometric Zn^{2+} imaging in live zebrafish larvae and estimate the chelatable Zn^{2+} level of the neuromasts in the larva head for the first time.

We thank the National Basic Research Program of China (No. 2011CB935800), National Natural Science Foundation of China (No. 21271100, 21131003, 21021062, and 91213305) for financial support. Z. Liu thanks the support from the Natural Science Foundation of Shandong Province (ZR2011BQ010). C. Zhang thanks the support from the Jiangsu Planned Projects for Postdoctoral Research Founds (No.1301005C).

Notes and references

1 (*a*) J. M. Berg and Y. Shi, *Science*, 1996, **271**, 1081; (*b*) M. Lu and D. Fu, *Science*, 2007, **317**, 1746.
2 (*a*) C. J. Frederickson, J.-Y. Koh and A. I. Bush, *Nat. Rev. Neurosci.*, 2005, **6**, 449; (*b*) M. Cortesi, R. Chechik, A. Breskin, D. Vartsky, J. Ramon, G. Raviv, A. Volkov and E. Fridman, *Phys. Med. Biol.*, 2009, **54**, 781.
3 (*a*) E. Tomat and S. J. Lippard, *Curr. Opin. Chem. Biol.*, 2010, **14**, 225; (*b*) Z. Xu, J. Yoon and D. R. Spring, *Chem. Soc. Rev.*, 2010, **39**, 1996; (*c*) E. L. Que, D. W. Domaille and C. J. Chang, *Chem. Rev.*, 2008, **108**, 1517; (*d*) P. Jiang and Z. Guo, *Coord. Chem. Rev.*, 2004, **248**, 205.
4 (*a*) S. Ellingsen, M. A. Laplante, M. Konig, H. Kikuta, T. Furmanek, E. A. Hoivik and T. S. Becker, *Development*, 2005, **132**, 3799; (*b*) H. W. Detrich, M. Westerfield and L. I. Zon, *The zebrafish: disease models and chemical screens*, Academic Press, Waltham, 3rd edn, 2011; (*c*) L. A. Trinh and S. E. Fraser, *Dev., Growth Differ.*, 2013, **55**, 434; (*d*) S. Rinkwitz, P. Mourrain and T. S. Becker, *Prog. Neurobiol.*, 2011, **93**, 231; (*e*) S.-K. Ko, X. Chen, J. Yoon and I. Shin, *Chem. Soc. Rev.*, 2011, **40**, 2120.
5 (*a*) F. Qian, C. Zhang, Y. Zhang, W. He, X. Gao, P. Hu and Z. Guo, *J. Am. Chem. Soc.*, 2009, **131**, 1460; (*b*) Z. Xu, K.-H. Baek, H. N. Kim, J. Cui, X. Qian, D. R. Spring, I. Shin and J. Yoon, *J. Am. Chem. Soc.*, 2010, **132**, 601; (*c*) J. E. Kwon, S. Lee, Y. You, K.-H. Baek, K. Ohkubo, J. Cho, S. Fukuzumi, I. Shin, S. Y. Park and W. Nam, *Inorg. Chem.*, 2012, **51**, 8760; (*d*) K. Jobe, C. H. Brennan, M. Motevalli, S. M. Goldup and M. Watkinson, *Chem. Commun.*, 2011, **47**, 6036; (*e*) Y. Xu, Q. Liu, B. Dou, B. Wright, J. Wang and Y. Pang, *Adv. Healthcare Mater.*, 2012, **1**, 485.
6 (*a*) Z. Liu, W. He and Z. Guo, *Chem. Soc. Rev.*, 2013, **42**, 1568; (*b*) L. Xue, G. Li, D. Zhu, Q. Liu and H. Jiang, *Inorg. Chem.*, 2012, **51**, 10842; (*c*) L. Xue, G. Li, D. Zhu, C. Yu and H. Jiang, *Chem.–Eur. J.*, 2012, **18**, 1050; (*d*) Z. Liu, C. Zhang, Y. Chen, W. He and Z. Guo, *Chem. Commun.*, 2012, **48**, 8365.
7 H. M. Kim, M. S. Seo, M. J. An, J. H. Hong, Y. S. Tian, J. H. Choi, O. Kwon, K. J. Lee and B. R. Cho, *Angew. Chem., Int. Ed.*, 2008, **47**, 5167.
8 M. Taki, J. L. Wolford and T. V. O'Halloran, *J. Am. Chem. Soc.*, 2004, **126**, 712.
9 K. A. Grant, D. W. Raible and T. Piotrowski, *Neuron*, 2005, **45**, 69.